

# Evidence of a Broad Relativistic Iron Line from the Neutron Star Low-Mass X-ray Binary Serpens X-1

Sudip Bhattacharyya<sup>1,2</sup>, and Tod E. Strohmayer<sup>3</sup>

## ABSTRACT

We report on an analysis of *XMM-Newton* data from the neutron star low mass X-ray binary (LMXB) Serpens X-1 (Ser X-1). Spectral analysis of EPIC PN data indicates that the previously known broad iron  $K\alpha$  emission line from this source has a significantly skewed structure with a moderately extended red wing. The asymmetric shape of the line is well described with the `laor` and `diskline` models in XSPEC and strongly supports an inner accretion disk origin of the line. To our knowledge this is the first strong evidence of a relativistic line in a neutron star LMXB. This finding suggests that the broad lines seen in other neutron star LMXBs likely originate from the inner disk as well. Detailed study of such lines opens up a new way to probe neutron star parameters and their strong gravitational fields. The red wing of the iron line from Ser X-1 is not as broad as that observed from some black hole systems. This is not unreasonable for a neutron star system, as the accretion disk has to terminate at or before the hard stellar surface. Finally, the inferred source inclination angle in the approximate range  $40^\circ$ - $60^\circ$  is consistent with the lack of dips and eclipses from Ser X-1.

*Subject headings:* accretion, accretion disks — line: profiles — relativity — stars: neutron — X-rays: binaries — X-rays: individual (Serpens X-1)

## 1. Introduction

The bright persistent LMXB Ser X-1 was discovered in 1965 (Bowyer et al. 1965). The detection of type I X-ray bursts from this source established that it harbors a neutron star

---

<sup>1</sup>CRESST and X-ray Astrophysics Lab, Astrophysics Science Division, NASA's Goddard Space Flight Center, Greenbelt, MD 20771; sudip@milkyway.gsfc.nasa.gov

<sup>2</sup>Department of Astronomy, University of Maryland, College Park, MD 20742

<sup>3</sup>X-ray Astrophysics Lab, Astrophysics Science Division, NASA's Goddard Space Flight Center, Greenbelt, MD 20771; stroh@clarence.gsfc.nasa.gov

(Swank et al. 1976; Li et al. 1977), as such bursts originate from the thermonuclear burning of matter on the stellar surfaces (Woosley & Taam 1976; Lamb & Lamb 1978; Strohmayer & Bildsten 2006). The lack of energy dependent dips and eclipses in the X-ray light curve of Ser X-1 suggests that its inclination angle may be less than  $60^\circ$  (Frank et al 1987; White & Swank 1982). The analysis of *RXTE* and *BeppoSAX* data revealed that the continuum spectra could be well fitted with a combination of absorbed Comptonization and disk blackbody models (Oosterbroek et al. 2001). Moreover, these authors reported the existence of a broad iron emission line near 6 keV, which they could adequately fit with a Gaussian model. Broad iron emission lines (near 6 keV) have been observed from many LMXBs (Asai et al. 2000; Bhattacharyya et al. 2006; Miller et al. 2002a), and active galactic nuclei (AGN; Reynolds & Nowak 2003). These lines could be broadened by either Doppler and relativistic effects (due to Keplerian motion in the inner accretion disk; Fabian et al. 1989), or Compton scattering (in a disk corona; Misra & Kembhavi 1998). It has also been suggested recently that complex absorption from perhaps several ionized components may partially account for some of the broad line component (e.g., Turner et al. 2005). The *ASCA* data from the Seyfert-1 galaxy MCG-6-30-15 gave the first strong clues that such lines originate in the inner accretion disk, as the high signal-to-noise ratio data revealed a skewed and double-horned profile, consistent with Doppler and relativistic effects in the inner accretion disk, where the speed of matter is a substantial fraction of the speed of light (Tanaka et al. 1995). Analysis of more recent data has strongly supported this inner disk origin of the line for MCG-6-30-15 and other AGN (Reynolds & Nowak 2003; Wilms et al. 2001; Reynolds et al. 2004; Reeves et al. 2007; Miniutti et al. 2007). Such lines, therefore, are extremely useful probes of strong gravity, and black hole properties, including spin (Brenneman & Reynolds 2006).

An inner disk origin has also been suggested for broad lines in some stellar mass black hole binaries, such as Cyg X-1 and GRS 1650–500 (Miller et al. 2002a; 2002b; Fabian et al. 1989). But, the origin of the broad iron lines from neutron star LMXBs has not been as well understood. This is largely because the available data have a modest signal-to-noise ratio, which was not precise enough to rule out simple symmetric profiles (such as a Gaussian profile). If the inner accretion disk origin can be established for broad iron lines from neutron star LMXBs, then the shape and width of the line may be used to constrain the radius of the inner edge of the disk, as well as the Keplerian speed at that radius. The former can give an upper limit to the neutron star radius (as the disk inner edge radius must be greater than or equal to the stellar radius), while both quantities may be utilized to constrain the stellar mass. Moreover, high frequency quasi-periodic oscillations (kHz QPOs) are observed from many neutron star LMXBs (van der Klis 2006). Although the actual physical mechanism responsible for these timing features is still debated, the leading models involve strong gravity, with the accretion disk close to the neutron star surface. Therefore,

if the inner disk origin can be established, the broad iron lines can be useful to constrain kHz QPO models, and together these two spectral and timing features will be extremely important as probes of strong gravity, and to constrain neutron star parameters. We note that the constraints on neutron star mass and radius can be useful to determine the equation of state (EoS) of high density cold matter at the stellar core, which is a fundamental problem of physics (see Bhattacharyya et al. 2005). In this Letter, we present evidence for an inner accretion disk origin of the broad iron line from the neutron star LMXB Ser X-1. In § 2, we describe our analysis of *XMM-Newton* data, and in § 3 we discuss the implications of our results.

## 2. Spectral Analysis

The neutron star LMXB Ser X-1 was observed three times with *XMM-Newton* in March, 2004 (obsIds: 0084020401, 0084020501, 0084020601). These observations were each separated in time by two days, and each consists of about 22 ks of data. Due to the brightness of the source, there are no European Photon Imaging Camera (EPIC) MOS detector data available for these observations. EPIC PN data were obtained in timing mode, and the source photons were also registered by the Reflection Grating Spectrometer (RGS) instruments. However, as no significant source spectral lines were detected in the RGS energy range, here we report only the analysis of the EPIC PN spectra. We have excluded the portions of the EPIC PN data with high and variable background (due to soft proton flares), and extracted source spectra, background spectra, and response matrices using the *XMM-Newton* Science Analysis Software (SAS; version 3.0). The SAS task ‘epatplot’ has indicated that this set of spectra (set 1) is modestly piled up. We have, therefore, extracted another set of spectra (set 2) after excluding the contributions from the central (and hence the brightest) pixels in order to minimize the pile-up effect. Results from the two spectral sets are consistent with each other, and the broad double-peaked line, which is the focus of this Letter, is present in both sets in the same energy range. This is expected, as pile-up cannot generate a double-peaked line. Based on these findings we do not believe pile-up is a significant concern for our study. Therefore, we have used spectral set 1 because of its higher signal-to-noise ratio.

We have rebinned the spectra (see, for example, Ibarra et al. 2007), fitted them with various models (within XSPEC), and found that the best model to describe the observed continuum spectra consists of an absorbed Comptonization (`compTT`) component plus a disk blackbody (`diskbb`). The addition of `diskbb` to the `compTT` component is essential, as can be seen from Table 1. This is in accordance with observations of Ser X-1 obtained with other X-ray missions (see Oosterbroek et al. 2001). Oosterbroek et al. noted that the choice

between a disk blackbody and a single temperature blackbody was arbitrary, however, our spectral fitting shows that a disk blackbody is preferred to a simple blackbody. For example, the choice of the former reduces  $\chi^2$  by about 47 compared to that for the latter (obs. 1, i.e., obsId 0084020401). Such a decrease in  $\chi^2$  is significant, and a similar decrease is found for obs. 2 (obsId 0084020501) and obs. 3 (obsId 0084020601). Table 1 shows that the addition of a Gaussian emission line near 0.54 keV improves the fit very significantly. As we have not found any source spectral lines at this energy in the RGS data, we suspect that this feature may be of instrumental origin, so we have fixed the line centroid of this feature at  $\approx 0.54$  keV in our subsequent model fitting. Finally, we have found highly significant excess emission near 6 keV. As a broad iron emission line is detected near this energy from many LMXBs (see § 1), we have fitted this excess emission with a Gaussian. This extra component is very significant (see Table 1), consistent with the results reported in Oosterbroek et al. (2001). However, as we have mentioned in § 1, it is not yet known with any certainty what broadens this line for neutron star LMXBs. To explore this question in more detail we have replaced the 6 keV Gaussian component with the `diskline` model component of XSPEC. This component represents the spectral line emission from the inner portion of an accretion disk in the Schwarzschild spacetime (Fabian et al. 1989). The corresponding fits show that the `diskline` model describes the line profile significantly better than the simple Gaussian profile (see Table 1). This result supports the notion that the line is produced in the inner accretion disk. In order to further substantiate this result, we have also modeled the spectrum using the `laor` model. This model is similar to the `diskline` model, but it includes the effects of the spin of the central star (Laor 1991). The fact that the `laor` model also fits the line profile significantly better than the simple Gaussian (see Table 1) provides strong evidence of the inner disk origin of this line. In fact, `laor` describes the line profile slightly better than `diskline` (primarily for obs. 1; see table 1). However, while there is some indication of a smaller disk inner radius in the `laor` fit using obs. 1, a value of  $6r_g$  is not yet excluded with sufficient significance to argue that the spin of the neutron star is affecting the line profile. In principle, deeper observations could test for such an effect.

In Table 2, we give the best-fit parameter values for the XSPEC model `wabs*(compTT+diskbb+gauss+laor)` for each observation. These values are consistent across the three observations. Here we note that we have used the disk geometry for the Comptonizing plasma (`compTT` model). However, even the spherical geometry gives very similar parameter values, except for the `compTT` optical depth  $\tau_C$  (the latter geometry gives  $\tau_C \approx 15$ ). We have constrained the rest frame line energy ( $E_L$ ; `laor` component) in the range 6.4 – 6.97 keV while fitting. This is because,  $K\alpha$  spectral lines from neutral or ionized iron are expected in this range. However, although we have always found 6.4 keV as the best-fit value of  $E_L$ , relaxing this constraint does not lower the best-fit  $E_L$  much. We have found the best-fit source incli-

nation angle,  $i_L$ , in the range  $\approx 40^\circ - 60^\circ$ , which is consistent with the expected value ( $< 60^\circ$ ) for Ser X-1 (due to the lack of eclipses and dips; see § 1). Here we note that, since there are many model parameters, we have fixed the line parameters (except the normalizations) to their best-fit values to estimate the errors on the parameters of the `wabs`, `compTT`, and `diskbb` components. Similarly, we have frozen the parameters (except the normalizations) of the `compTT` and `diskbb` models in order to estimate the errors on the spectral line parameters. Therefore, the quoted error values are likely somewhat underestimated. Fig. 1 shows the data, model components, and data-to-model ratio for observation 2. The `laor` model component for the broad iron line is clearly shown by the double-peaked dotted line. The moderately structured shape of the data-to-model ratio results in a relatively high overall reduced  $\chi^2$  for Ser X-1 (Table 2). Note that similar residuals, and a high reduced  $\chi^2$  were also reported by Oosterbroek et al. (2001; see their Figs. 5 & 6). These authors argued that these narrow structures could not be caused by an incorrect continuum modeling, since such incorrectness would probably give more smoothly varying data-to-model ratios. Fig. 2 exhibits the structure of the broad relativistic iron line. The two panels show this line from two observations. The data points of the figure clearly show the line with an extended red wing. This figure also explicitly shows that both the `laor` model and the `diskline` model (dotted line in each panel) fit the spectral line profile well.

### 3. Discussion and Conclusions

In this Letter, we report the results of the spectral fitting of the *XMM-Newton* EPIC PN data from the neutron star LMXB Ser X-1. The best-fit continuum parameter values (see Table 2) are generally consistent with those of Oosterbroek et al. (2001). Our slightly higher Comptonization plasma temperature ( $T_C$ ) compared to that of Oosterbroek et al. can be explained in terms of the lower 2 – 10 keV flux that we have found. This is because, as the intensity of an LMXB decreases, its energy spectrum generally becomes harder.

It was previously known that Ser X-1 exhibits a broad iron line (see § 1), but earlier data did not have the statistical quality to rule out simple symmetric profiles (such as a Gaussian). As a result, its origin was not strongly constrained. Knowledge of the line’s origin is very important, because if it is produced in the inner accretion disk, it can be used (1) to probe the strong gravitational field of the neutron star, (2) to constrain the stellar parameters, and (3) to constrain models of the kHz QPOs, which may, in turn, be useful to achieve the first two goals (see § 1). By analyzing *XMM-Newton* EPIC PN data we have demonstrated that the line is significantly asymmetric, and can be accurately modeled with physical models of line formation in the inner disk (using the `diskline` and `laor` models

in XSPEC; see Fig. 2). This strongly supports the idea that this spectral line originates from the inner accretion disk of Ser X-1 (see § 1). The high signal-to-noise ratio data also revealed the detailed shape of the broad and relativistically skewed line with an extended red wing (Fig. 2). Such lines have so far been observed from AGNs and a few Galactic black hole X-ray binaries (Tanaka et al. 1995; Miniutti et al. 2007; Miller et al. 2002a; 2002b), but this is the first strong evidence of a relativistic line in a neutron star system. As we have mentioned in § 1, other neutron star LMXBs exhibit broad iron emission lines, which so far have been adequately modeled with simple Gaussian profiles. Our finding for Ser X-1 suggests that the lines seen in other LMXBs may also originate from the inner accretion disk, and its relativistically skewed nature could be confirmed with sufficiently long observations. If future observations bear this out it will open up an exciting new opportunity to probe neutron stars and strong gravity with deep spectroscopic observations.

We have found that the equivalent width ( $EW_L$ ) of the iron line from Ser X-1 is lower than that reported in Oosterbroek et al. (2001), which may suggest that the strength of this line decreases with the source intensity. The source inclination angle inferred from both the `diskline` and `laor` fits is consistent with  $\lesssim 60^\circ$ , which is expected for the non-dipping nature of Ser X-1 (see § 1). The best-fit values of  $R_{\text{in}}$  for obs. 1 & 3 (see Table 2) suggest that the accretion disk extends almost to the neutron star surface. Although this is not the case for obs. 2, it is to be noted that both the source count rate and the iron line strength are relatively low for this observation (Table 2), and hence the spectral line statistics are not as good as for the other two obsIDs. However, we cannot make a definite conclusion regarding the disk extension with the current data. But we note that the accretion disk can plausibly approach the neutron star surface because the stellar magnetic field in LMXBs is relatively low ( $\approx 10^{8-9}$  G), and the implied accretion rate for Ser X-1 is high ( $\approx 0.28 - 0.32\dot{M}_{\text{Edd}}$ ; based on the observed flux, and the Eddington luminosity  $\approx 2.0 - 3.8 \times 10^{38}$  ergs  $\text{s}^{-1}$ , for a distance of  $\approx 9.5 - 12.7$  kpc; Jonker & Nelemans 2004). An important difference between neutron star and black hole systems in the context of disk line formation is the presence of the neutron star surface. This sets a firm limit on the inner edge of the disk in a neutron star system, even a rapidly spinning one, although the exact limit will depend on the EoS of neutron star matter. For black holes, significant spin always implies a smaller disk inner edge radius (for a corotating disk). Therefore, for very fast spinning black holes, the red wing of the relativistic iron line is expected to be very broad. So the relatively modest extended red wing (compared to some black hole systems; Miniutti et al. 2007) of the iron line from Ser X-1 appears consistent with the fact that this source harbors a neutron star. This relativistic iron line is expected to be accompanied by a continuum reflection spectral component (Reynolds & Nowak 2003). A distinct feature of this component is a broad hump near 30 keV. As the signal-to-noise ratio of the EPIC PN data is small at higher energies

( $\geq 10$  keV), we could not determine if this component is present in the Ser X-1 spectra.

The authors thank Tim Kallman and Jean Cottam for useful discussions, and John Miller and an anonymous referee for helpful comments.

## REFERENCES

- Asai, K., Dotani, T., Nagase, F., & Mitsuda, K. 2000, *ApJSS*, 131, 571
- Bhattacharyya, S., Strohmayer, T. E., Swank, J. H., & Markwardt, C. B. 2006, *ApJ*, 652, 603
- Bhattacharyya, S., Strohmayer, T. E., Miller, M. C., & Markwardt, C. B. 2005, *ApJ*, 619, 483
- Bowyer, S., Byram, E. T., Chubb, T. A., & Friedman, H. 1965, *Science*, 147, 394
- Brenneman, L. W., & Reynolds, C. S. 2006, *ApJ*, 652, 1028
- Fabian, A. C., Rees, M. J., Stella, L., & White, N. E. 1989, *MNRAS*, 238, 729
- Frank, J., King, A. R., & Lasota, J.-P. 1987, *A&A*, 178, 137
- Ibarra, A. et al. 2007, *A&A*, 465, 501
- Jonker, P. G., & Nelemans, G. 2004, *MNRAS*, 354, 355
- Lamb, D. Q., & Lamb, F. K. 1978, *ApJ*, 220, 291
- Laor, A. 1991, *ApJ*, 376, 90
- Li, F. K. et al. 1977, *MNRAS*, 179, 21
- Miller, J. M. et al. 2002a, *ApJ*, 578, 348
- Miller, J. M. et al. 2002b, *ApJ*, 570, L69
- Miniutti, G. et al. 2007, *PASJ*, 59, S315
- Misra, R., & Kembhavi, A. K. 1998, *ApJ*, 499, 205
- Oosterbroek, T., Barret, D., Guainazzi, M., & Ford, E. C. 2001, *A&A*, 366, 138
- Reeves, J. N. et al. 2007, *PASJ*, 59, 301

- Reynolds, C. S., & Nowak, M. A. 2003, *Physics Reports*, 377, 389
- Reynolds, C. S., Wilms, J., Begelman, M. C., Staubert, R., & Kendziorra, E. 2004, *MNRAS*, 349, 1153
- Strohmayer, T. E., & Bildsten, L. 2006, in *Compact Stellar X-ray Sources*, Eds. W.H.G. Lewin and M. van der Klis, (Cambridge University Press: Cambridge), 113
- Swank, J. H., Becker, R. H., Pravdo, S. H., & Serlemitsos, P. J. 1976, *IAU Circ.*, 2963
- Tanaka, Y. et al. 1995, *Nature*, 375, 659
- Turner, T. J., Kraemer, S. B., George, I. M., Reeves, J. N., & Bottorff, M. C. 2005, *ApJ*, 618, 155
- van der Klis, M. 2006, in *Compact Stellar X-ray Sources*, Eds. W.H.G. Lewin and M. van der Klis, (Cambridge University Press: Cambridge), 39
- White, N. E., & Swank, J. H. 1982, *ApJ*, 253, L61
- Wilms, J. et al. 2001, *MNRAS*, 328, L27
- Woosley, S. E., & Taam, R. E. 1976, *Nature*, 263, 101



Table 1. Fitting of the *XMM-Newton* EPIC PN energy spectra from Ser X-1 with various XSPEC models.

No.	XSPEC Model	$\chi^2/\text{dof}^a$ (Obs. 1 <sup>b</sup> )	$\chi^2/\text{dof}^a$ (Obs. 2 <sup>b</sup> )	$\chi^2/\text{dof}^a$ (Obs. 3 <sup>b</sup> )
1	wabs*compTT	$\frac{2689.1}{706}$	$\frac{2517.2}{706}$	$\frac{2464.3}{706}$
2	wabs*(compTT+diskbb)	$\frac{1708.9}{704}$ (0)	$\frac{1198.0}{704}$ (0)	$\frac{1432.5}{704}$ (0)
3	wabs*(compTT+diskbb+gauss)	$\frac{1517.6}{702}$ (8.0E-19)	$\frac{1103.8}{702}$ (3.3E-13)	$\frac{1338.2}{702}$ (4.2E-11)
4	wabs*(compTT+diskbb+gauss+gauss)	$\frac{1192.7}{699}$ (2.7E-36)	$\frac{949.1}{699}$ (9.7E-23)	$\frac{1098.0}{699}$ (8.4E-30)
5	wabs*(compTT+diskbb+gauss+diskline)	$\frac{1165.6}{696}$ (1.1E-3)	$\frac{917.4}{696}$ (3.0E-5)	$\frac{1068.9}{696}$ (3.1E-4)
6	wabs*(compTT+diskbb+gauss+laor)	$\frac{1153.6}{696}$ (3.6E-5)	$\frac{917.8}{696}$ (3.4E-5)	$\frac{1060.5}{696}$ (2.3E-5)

<sup>a</sup>The number in the parentheses is the probability (calculated from F-test using XSPEC) of the decrease of  $\chi^2/\text{dof}$  by chance from the value of the previous row to that of the current row (for models 2 – 5). For model 6, the comparison is with model 4. A very small value is replaced with a zero.

<sup>b</sup>Obs. 1: ObsId 0084020401; Obs. 2: ObsId 0084020501; Obs. 3: ObsId 0084020601.

Table 2. Best fit parameters (with 90% confidence) for the *XMM-Newton* EPIC PN energy spectra from Ser X-1.

Parameter <sup>a</sup>	Obs. 1 <sup>b</sup>	Obs. 2 <sup>b</sup>	Obs. 3 <sup>b</sup>
$N_{\text{H}}^{\text{c}}$ ( $10^{22}$ atoms $\text{cm}^{-2}$ )	$0.48^{+0.02}_{-0.02}$	$0.44^{+0.01}_{-0.01}$	$0.49^{+0.02}_{-0.02}$
$T_0^{\text{d}}$ (keV)	$0.17^{+0.01}_{-0.01}$	$0.19^{+0.01}_{-0.01}$	$0.17^{+0.02}_{-0.01}$
$T_{\text{C}}^{\text{e}}$ (keV)	$3.18^{+0.54}_{-0.36}$	$2.63^{+0.14}_{-0.11}$	$2.81^{+0.35}_{-0.18}$
$\tau_{\text{C}}^{\text{f}}$	$6.19^{+0.68}_{-0.74}$	$7.25^{+0.30}_{-0.32}$	$6.71^{+0.48}_{-0.52}$
$T_{\text{in}}^{\text{g}}$ (keV)	$1.71^{+0.10}_{-0.12}$	$1.21^{+0.04}_{-0.04}$	$1.40^{+0.08}_{-0.08}$
$E_{\text{L}}^{\text{h}}$ (keV)	$6.40^{+0.08}_{-0.0}$	$6.40^{+0.03}_{-0.0}$	$6.40^{+0.04}_{-0.0}$
$\beta_{\text{L}}^{\text{i}}$	$2.17^{+0.30}_{-0.13}$	$2.38^{+0.31}_{-0.56}$	$2.55^{+0.39}_{-0.30}$
$R_{\text{in}}^{\text{j}}$	$4.04^{+2.14}_{-0.68}$	$16.19^{+8.77}_{-3.19}$	$5.59^{+1.48}_{-1.19}$
$R_{\text{out}}^{\text{k}}$	$271.5^{+115.2}_{-93.7}$	$400.0^{+0.0}_{-70.9}$	$313.5^{+86.5}_{-166.9}$
$i_{\text{L}}^{\text{l}}$ (degree)	$44.7^{+1.7}_{-3.2}$	$50.2^{+8.8}_{-5.4}$	$39.7^{+1.4}_{-1.5}$
$EW_{\text{L}}^{\text{m}}$ (eV)	$105.1^{+6.8}_{-8.0}$	$85.9^{+8.9}_{-10.8}$	$95.2^{+11.6}_{-8.9}$
$\chi^2/\text{dof}$	1153.6/696	917.8/696	1060.5/696
Flux <sup>n</sup> (0.5 – 2 keV)	0.93	0.87	0.91
Flux <sup>n</sup> (2 – 10 keV)	4.22	3.34	3.79

<sup>a</sup>Parameters of the XSPEC model `wabs*(compTT+diskbb+gauss+laor)`.

<sup>b</sup>Obs. 1: ObsId 0084020401; Obs. 2: ObsId 0084020501; Obs. 3: ObsId 0084020601.

<sup>c</sup>Hydrogen column density from the `wabs` model component.

<sup>d</sup>Input soft photon (Wien) temperature of the `compTT` model component.

<sup>e</sup>Temperature of the Comptonizing plasma (`compTT` model component; disk geometry).

<sup>f</sup>Optical depth of the Comptonizing plasma (`compTT` model component).

<sup>g</sup>Temperature at inner disk radius from `diskbb` model component.

<sup>h</sup>Rest frame energy of the broad relativistic iron emission line (`laor` model component).

<sup>i</sup>Power law index of emissivity (`laor` model component).

<sup>j</sup>Inner radius (in the unit of  $GM/c^2$ ;  $M$  is the mass of the neutron star) from the `laor` model component.

<sup>k</sup>Outer radius (in the unit of  $GM/c^2$ ) from the `laor` model component.

<sup>l</sup>Source inclination angle from the `laor` model component.

<sup>m</sup>Equivalent width of the broad relativistic iron emission line (`laor` model component).

<sup>n</sup>Observed flux in  $10^{-9}$  ergs  $\text{cm}^{-2}$   $\text{s}^{-1}$ .

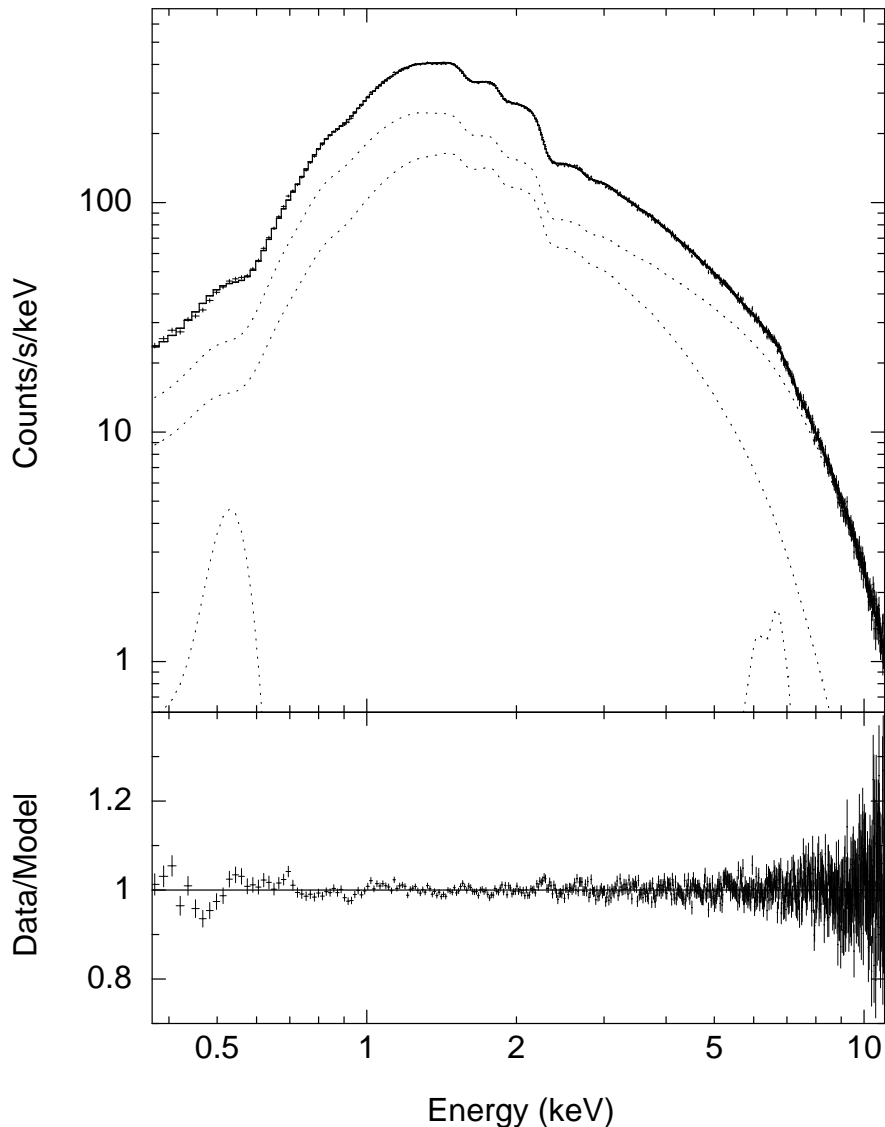


Fig. 1.— *XMM-Newton* EPIC PN energy spectrum from Ser X-1 for obs. 2 (obsId 0084020501). The upper panel shows the data (error bars), model (solid line), and individual additive model components (dotted lines). Here we have used the best-fit XSPEC model `wabs*(compTT+diskbb+gauss+laor)` (see Table 2). Among the two continuum additive model components, the upper dotted line shows `compTT`, and the lower dotted line shows `diskbb`. The low energy emission line is the `gauss` component, while the high energy broad iron emission line is the `laor` component. The lower panel shows the data to model ratio.

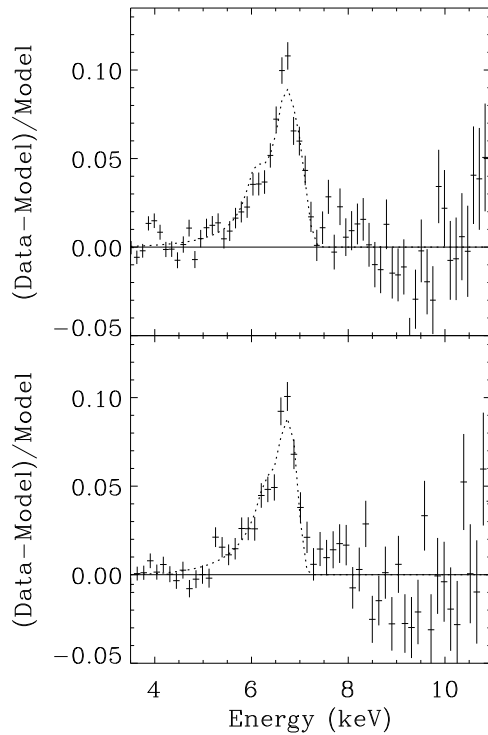


Fig. 2.— *Upper panel:* *XMM-Newton* EPIC PN energy spectrum from Ser X-1 for obs. 1 (obsId 0084020401). With the error bars we show the data intensity in excess of the model intensity, and normalized by the model intensity (i.e.,  $(\text{Data}-\text{Model})/\text{Model}$ ). Here the model is the best-fit model (of Table 2) minus the `laor` component. The `laor` component is separately shown with the dotted line. *Lower panel:* Similar to the upper panel, but for obs. 3 (obsId 0084020601), and for the `diskline` component (model 5 of Table 1) instead of the `laor` component. For each panel, the data points clearly show a broad relativistic iron emission line with an extended red wing.